NIOBIUM SPUTTER-COATED COPPER RESONATORS

C. Benvenuti, S. Calatroni, I. E. Campisi[1], P. Darriulat, C. Durand[2], M. Peck, R. Russo, A.-M. Valente

CERN, CH-1211 Geneva 23, Switzerland

[1] On leave from TJNAF, Newport News, Virginia, 23606, USA

[2] Present address: INFN, Laboratori Nazionali di Legnaro, I-35020 Legnaro PD, Italy

Abstract

Niobium sputter-coated copper resonators are successfully employed in operating particle accelerators, the most outstanding example being LEP2 at CERN. In this review we present recent progress in the understanding of the basic principles governing their behaviour, based on an extensive R&D programme carried out at CERN on 1.5 GHz resonators operated in the TM_{010} mode. At the present stage of the study, no fundamental limitation has been found which would prevent the use of this technology for future high-field, high-Q accelerating cavities.

Introduction

Superconducting accelerating cavities are widely employed today in particle accelerators, both for their ability to provide beams of a quality not attainable with copper structures, and for the lower overall operating cost [1]. These cavities are manufactured essentially from bulk niobium, the most notable exception being the 352 MHz cavities for LEP2 at CERN. In this case, the choice has been made to employ niobium-coated copper cavities, following the successful development of the technology of sputter deposition of niobium films inside copper resonators [2]. This technology is now widely recognised as being a valid and in some cases superior alternative to bulk niobium resonators, and is being actively pursued in many research laboratories [3]. As is the case for bulk niobium, however, the niobium on copper technology still suffers from some limitations that prevent the exploitation of the superconducting material up to its theoretical physical limit.

An extensive R&D programme is being carried out at CERN, to better understand the physical mechanism governing the behaviour of thin niobium films in a high intensity RF field. The research has been focused onto coating a large number of different 1.5 GHz

resonators operated in the TM_{010} mode, and correlating the basic coating and material parameters to measured RF superconducting properties.

Experimental method

The resonators are constructed of Oxygen-Free Electronic grade (OFE) copper, which provides a substrate with an impurity content in the ppm range. The cavity construction technique has a profound effect on the structural properties of the copper substrate, which in turn may affect the growth and/or the purity of the niobium film. The need to avoid welds in the high field region of the cavity in order to reduce any uncertainty due to the presence of a molten section of the substrate, suggests the use of seamless cavities. These are manufactured by two different methods, namely hydroforming [4] and spinning [5]. Hydroformed cavities are produced by inflating at high pressure a copper tube inside a mould, with three intermediate annealing steps at 600 °C. The resulting cavity surface has a grain size of a few hundred microns, and an average roughness of the order of one micron. Spun cavities are produced by shaping a 3 mm copper sheet around a special collapsible mandrel, which can then be removed from the inside. The copper sheet is annealed at 250 °C before the spinning process, but no annealing takes place afterwards. The resulting copper grain size is smaller, and so is the average roughness.

The inner surface of the cavities is prepared for coating using the same polishing solution developed for LEP2 cavities [6]. Other methods such as electropolishing are being actively investigated. It has been proven by material analysis that after being shaped, the inner surface of the cavities is damaged and some copper must be removed to obtain a suitable surface. At least 120 μm of copper must be removed from spun cavities, whereas 40 μm are generally sufficient for hydroformed ones.

The sputtering niobium cathode is assembled in a class 100 clean room, where it is always kept when not in use. After coating, the niobium layer can be etched away, and the copper substrate can be used again for a subsequent coating after a light (10 μm to 20 μm) chemical polishing. High pressure water rinsing with ultra high purity water at 100 bar is performed before each deposition and before each RF measurement.

The coating method follows closely the sputtering procedure developed for LEP2, based on a cylindrical magnetron configuration, and adapted to 1.5 GHz cavities [7], as illustrated in figure 1. In a noble gas atmosphere, generally argon, at a pressure of 1.5×10^{-3} mbar, a potential difference is established between the central cathode and the grounded cavity. The electrical current of the glow discharge is stabilised at 3 A, resulting in a voltage of approximately 360 V depending on the magnetic induction of the permanent magnet. The sputter-coating takes place usually at 150 °C, and the coating thickness is 1.5 μm obtained after 15 minutes of treatment. The cut-off tubes are coated first, with slightly modified parameters: 10^{-2} mbar, 1 A, 320 V.

Extensive material analyses of samples cut from a spun cavity coated with these standard parameters have been carried out. The films have a Residual Resistivity Ratio (RRR) of 11±1, measured after dissolving the copper substrate in nitric acid. The average grain size is 100±50 nm, as measured by TEM in plane views close to the film surface. The argon

content, due to the sputtering process, has been measured by thermal extraction to be 400 ppm. X-ray diffraction analysis shows that the film grows preferentially in the <1,1,0> direction with an expanded lattice parameter [8], producing an increase in T_c.

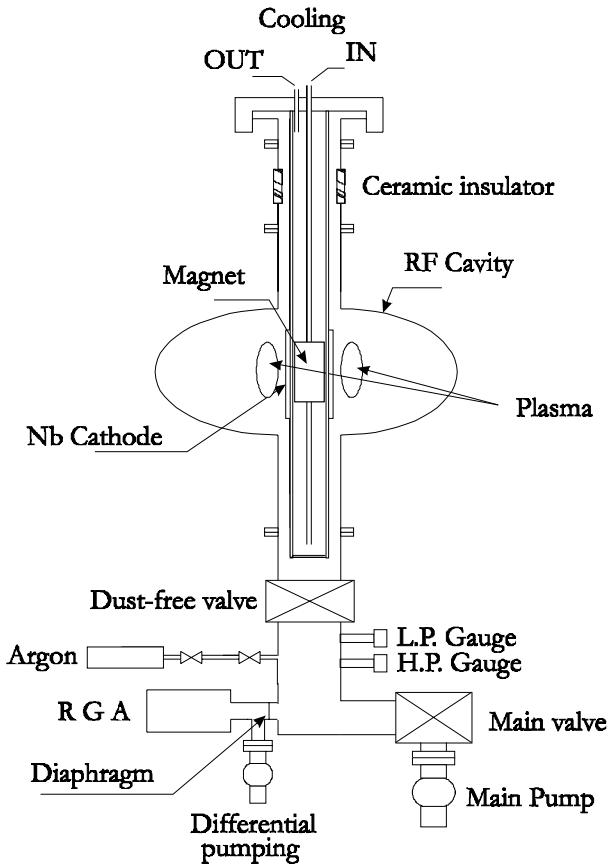

Figure 1. Schematic drawing of the 1.5 GHz single-cell cavity sputtering system.

The kind of noble gas used for sputtering, the temperature of the coating and its thickness are some of the variables that influence all these quantities, and their variation has been explored in detail throughout this project. In the following, we will however concentrate mainly on the analysis of the results obtained with 28 standard coatings (i.e. produced with the coating parameters described above).

As a reference, bulk niobium cavities produced either by spinning (courtesy of INFN-LNL) or by deep drawing (courtesy of TJNAF) have also been measured to compare our results with a known standard. The nominal RRR of the niobium employed for their fabrication is 300.

RF characterisation

The RF measurements are performed with a relatively standard RF system, in a liquid helium cryostat. Fixed antennas are used to couple the RF power in and out the cavity.

Temperature scans are performed between 4.2 K and 1.7 K, and the surface resistance is measured as a function of the RF field amplitude. Since the surface resistance at 4.2 K is much higher than at 1.7 K, the two measurements give almost uncorrelated measurements of the BCS surface resistance and of the residual resistance. The temperature dependence of the various components is then easily extracted.

A particularity of the present study is the systematic measurement of the surface resistance when an external magnetic flux is trapped into the film when crossing the superconducting transition. This measurement gives hints about the effect of localised defects (the pinning centres for the trapped fluxoids) on the surface resistance. Film cavities always show complete trapping, contrary to bulk cavities where trapping is incomplete in cavities fired at high temperature (~1000°C). The superconducting critical temperature can also be measured through the observation of the transition from the Meissner state.

The penetration depth can be computed by measuring the frequency shift as a function of temperature, normalised to the frequency shift of bulk niobium used as a clean limit reference ($\ell/\xi_0 \sim 20$). The penetration depth is in turn linked to the electron mean free path through the formula $\lambda(\ell)=\lambda_{CLEAN}(1+\pi\xi_0/2\ell)^{½}$

An approximate evaluation of the lower critical field H_{c1} is made by using a small superconducting coil placed in the cryostat at the equator of the cavity, and by measuring the value of the punch-through field at which the surface resistance starts increasing. Since the field lines are distorted by the presence of the cavity it is only possible to perform relative measurements, and the results must be normalised to the value measured for bulk niobium.

Discussion

In order to better understand the physical phenomena governing the surface resistance of the superconductors under study, it is convenient to separate it in three additive terms:

$$R_s(H_{RF}, H_{ext}, T) = R_{BCS}(H_{RF}, T) + R_{res}(H_{RF}) + R_{fl}(H_{RF}, H_{ext}, T)$$

The first term, the BCS surface resistance, is found to depend both on temperature and RF field amplitude. The second term, the residual resistance, which depends only on the field amplitude by definition, is to some extent out of control of the experiment as will be shown below. The last term expresses the dependence on external magnetic flux.

BCS resistance

The predictions by the BCS theory of the temperature and frequency dependence of the surface resistance have been extensively confirmed by experimental evidence [9], in particular for bulk niobium. Less data exist for the dependence of the surface resistance on the electron mean free path. No comprehensive calculations, nor systematic data exists on the other hand for the RF field dependence of the BCS surface resistance. It is therefore important to assess the behaviour for niobium thin films, where the electron mean free path can easily be tuned by varying the deposition parameters.

In this work it has been chosen to factorise the BCS resistance as the product of two terms, one depending only on T and the other only on H_{RF}: $R_{BCS}(H_{RF}, T) = R^0_{BCS}(T)\ G(H_{RF})$. The validity of this factorisation is proven in figure 2, where isothermal scans of R_{BCS} at various temperatures for a particular cavity are plotted in logarithmic scale. The fact that the lines are parallel shows indeed that the RF field dependence is the same, the curves differing only by a multiplicative factor.

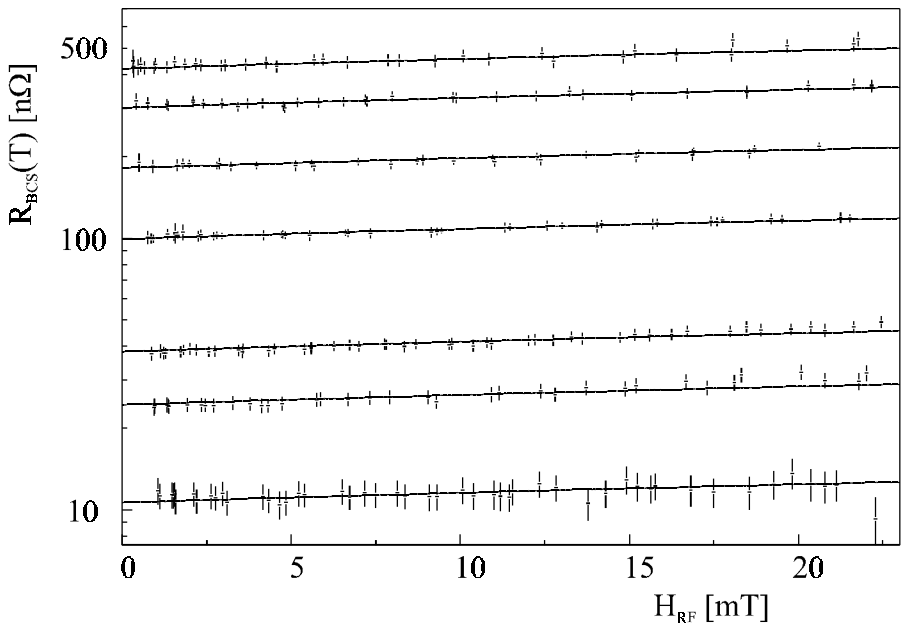

Figure 2. Isothermal scans of H_{RF} on a particular film. $R_{BCS}(T)$ is plotted as a function of H_{RF} for (from top to bottom) T= 4.23 K, 3.90 K, 3.47 K, 3.07 K, 2.59 K, 2.41 K, 2.15 K.

The temperature dependent factor $R^0_{BCS}(T)$ is consistent with BCS theory. Figure 3 shows its variation as a function of temperature for the 28 standard films, normalised to the value at 4.2 K. An exponential dependence can be used to fit an approximate value for the superconducting energy gap, equal to 19.6 K in temperature units. This value together with the average critical temperature of 9.54 K gives a coupling parameter α=2.05.

The actual value of R_{BCS} depends strongly on the electron mean free path [10]. Since ℓ/ξ_0 is estimated to be about 0.7 for our films, compared to about 20 for the bulk, it is not surprising that the BCS surface resistance of bulk niobium is more than double that for films (~900 nΩ compared to ~400 nΩ at zero RF field). This is illustrated in figure 4, from which one can also infer that the RF field dependent factor $G(H_{RF})$ is approximately equal for bulk and for film.

Residual resistance

The measurement of the BCS surface resistance confirms that the basic superconducting properties of the films are well understood. On the other hand, the ultimate goal of the study is the understanding of the factors governing the residual resistance. At the present stage, the residual resistance is under control only at the level of a few tens of nΩ. Many phenomena can have an influence on the residual resistance. One notable example is the

nature of the substrate, as illustrated in figure 5. Spun cavities seem to provide on average better results than hydroformed cavities, both in terms of R_{res} and of its increase with RF field. The most apparent difference between the two kinds of substrates is surface roughness. No clear mechanism relates roughness to residual resistance, although it may be speculated that this influences the film crystalline structure.

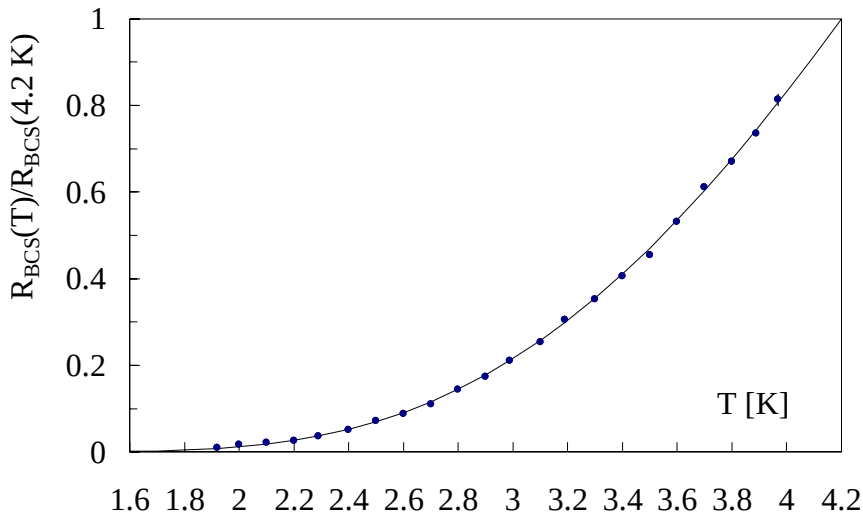

Figure 3. Average temperature dependence of $R_{BCS}(T)/R_{BCS}(4.2\ K)$ for 28 standard films. The line is the best fit of an exponential temperature dependence for $R_{BCS}(T)$.

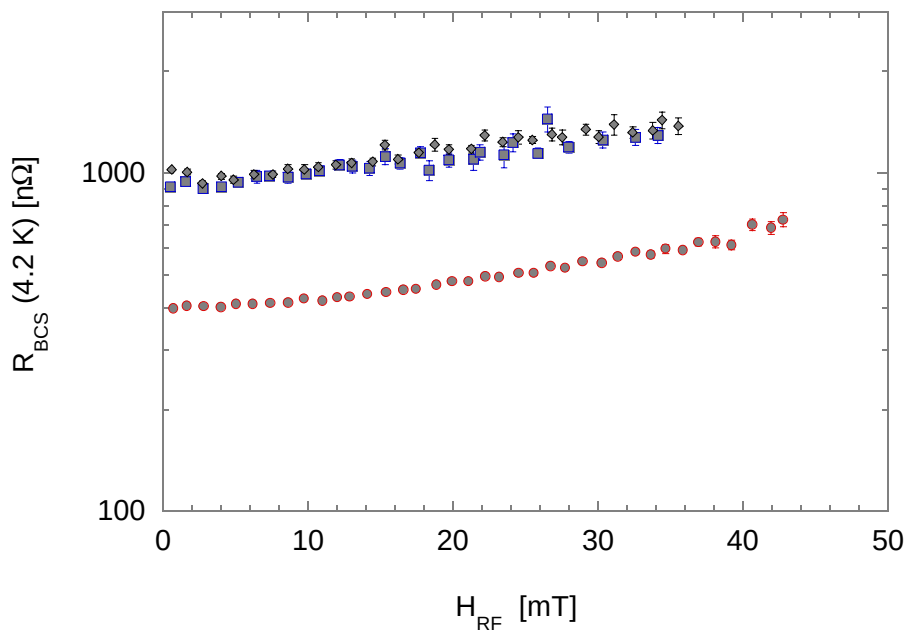

Figure 4. Dependence of $R_{BCS}(4.2\ K)$ on H_{RF} for film (rounds) and bulk cavities, as received (squares) and vacuum fired (diamonds). Error bars include the spread from different cavities.

It must be noted that cavities with very low residual resistance over a broad range of RF field can at times be produced. This provides evidence against the conjecture that the small grain size would be a fundamental limitation in the use of film cavities [11]. Figure 6 shows a few such examples, together with a bulk cavity as a reference. All the measurements have been stopped well below the field threshold for electron emission, but in some cases this threshold is quite high. No systematic attempt was made to optimise the high pressure water rinsing procedure in order to attain high maximum fields in the cavities. However, accelerating fields in excess of 15 MV/m have been repeatedly obtained, supporting the hypothesis that films behave no differently from bulk in this respect.

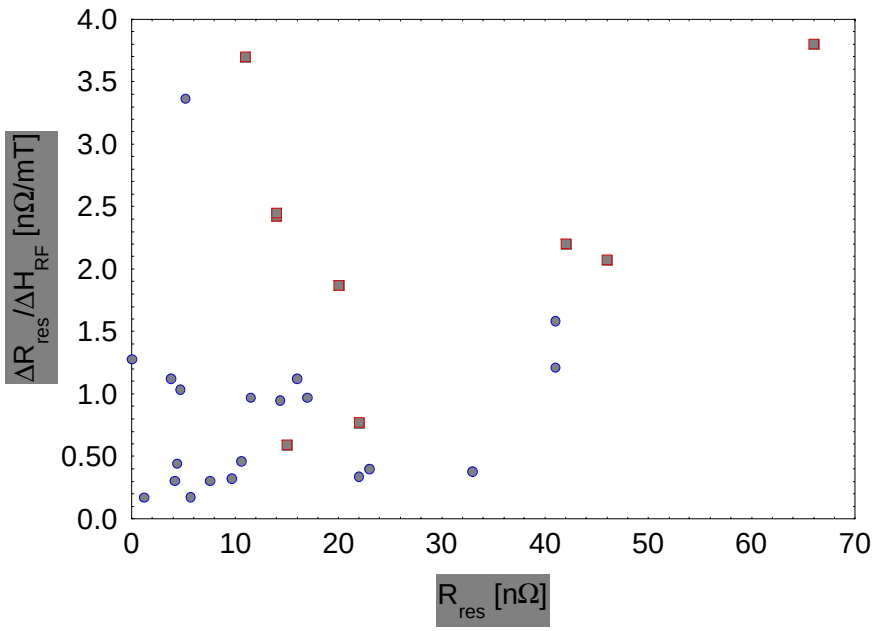

Figure 5. Slope at 1.7 K plotted as a function of R_{res} for 28 standard cavities. The slope is arbitrarily calculated by a linear extrapolation of the $R_s(H_{RF})$ behaviour at low field and up to a few tens of mT, varying for each cavity. Hydroformed cavities are represented by squares, spun cavities by round symbols.

Fluxon-induced surface resistance

Magnetic fluxes up to a few Gauss are used to measure the fluxon-induced surface resistance. It is experimentally proven that this quantity obeys, within reasonable limits, a bilinear relation of the form $R_{fl}=(R_{fl}^{0}+R_{fl}^{1}H_{RF})H_{ext}$. Although some models exist for the theoretical dependence on an external magnetic field, few descriptions correlate this dependence with the RF field amplitude.

The two quantities R_{fl}^{0} and R_{fl}^{1} turn out to be very sensitive to variations in purity. The difference between bulk niobium and standard films is extremely remarkable, with values of R_{fl}^{0} of 4.8 $n\Omega G^{-1}$ for films and 127 $n\Omega G^{-1}$ for bulk. On the other hand, R_{fl}^{1} does not change much, being about 1.15 $n\Omega G^{-1}mT^{-1}$ in both cases.

A more detailed analysis of fluxon induced losses, together with a complete report of all the measurements described herein, will be published in a forthcoming paper.

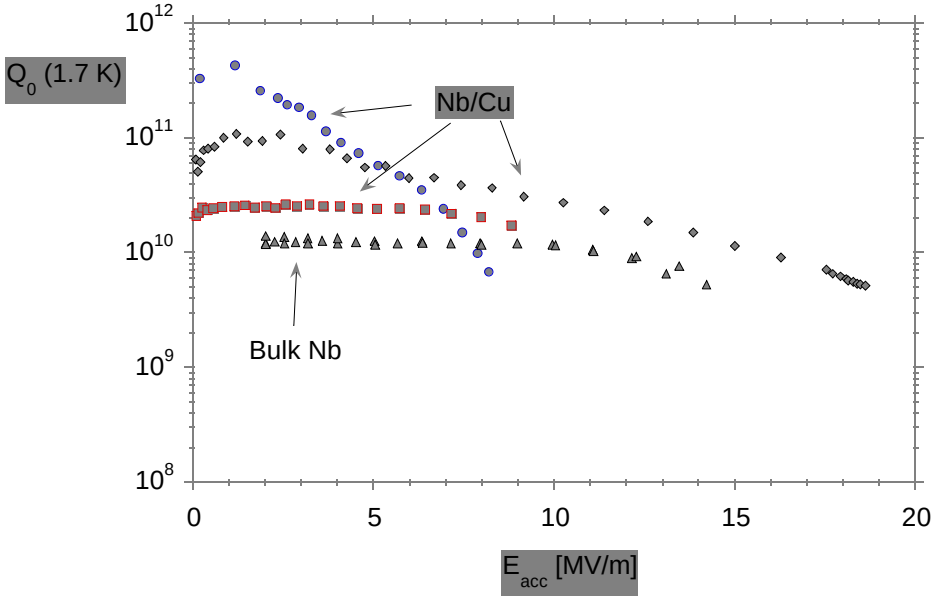

Figure 6. Q vs. H_{RF} curves for three Nb/Cu cavities, and a deep-drawn bulk niobium for comparison. The Q values have been measured at 4.2 K.

Penetration depth and H_{c1}

Both the penetration depth and the lower critical field H_{c1} depend on the electron mean free path ℓ. By changing the mass of the noble gas used for the sputtering process, or using mixtures of two gases in various proportions, one can tune the quantity of sputter gas atoms trapped in the film, and in turn ℓ. Figure 7 shows the comparison of measurements of the normalised values of H_{c1} and λ for cavities coated with various gases, indicating that the mean free path can effectively be changed in this way [12].

Conclusions

The standard coating procedure gives excellent and reproducible results, in terms of BCS parameters. New procedures for fine analysis of RF data have been set-up, which allow the distinction of subtle differences among coatings. On this basis, it will now be possible to explore all the phase space of the coating parameters in order to pinpoint those variables which are less understood, and which may affect the residual resistance.

One possible such candidate is the study of the interface between copper and niobium, that can be studied either by sputter-etching of the copper substrate, or by the deposition of a suitable interlayer.

A global discussion of these investigations will be available in the near future.

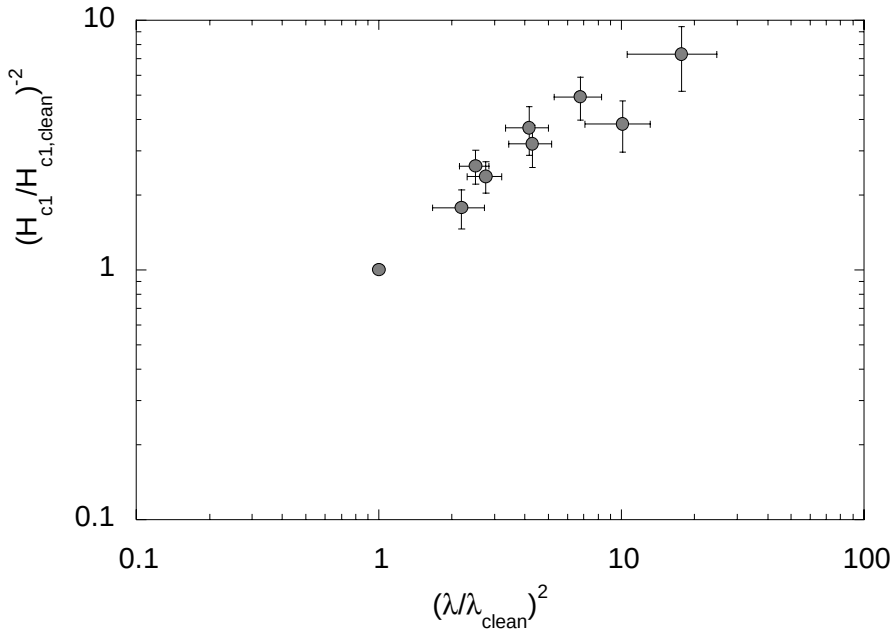

Figure 7. Comparison of penetration depth λ and H_{c1} measurements, normalised to the values of the clean limit (bulk niobium). Higher values correspond to shorter mean free paths.

Acknowledgements

The authors would like to thank V. Palmieri of LNL-INFN for providing spun copper and niobium cavities; P. Kneisel of TJNAF for providing deep-drawn niobium cavities and for measurements; S. Bauer and S. Forel for chemical treatments; F. Scalambrin for help with film coatings; S. Marsh and S. Sgobba for metallurgical analyses; N. Rensing and A. Cassinese for participation in the early part of the study; G. Cavallari, E. Haebel, E. Mahner, W. Weingarten for useful discussions; J. M. Rieubland and his staff for support in the Cryogenics Laboratory of CERN.

References

[1] H. Padamsee et al., Ann. Rev. Nucl. Part. Sci. 43 (1993) 635

[2] C. Benvenuti, Part. Accel. 40 (1992) 43

[3] Proceedings of the 8th Workshop on RF Superconductivity, Abano Terme, Italy, 1997

[4] V. Palmieri et al., paper presented at 4th Topical Symposium on Superconductivity and Superconducting Materials Technologies, Firenze, Italy, 1994

[5] C. Hauviller, paper presented at the IEEE Particle Accelerators Conference, Chicago IL, USA, 1989

[6] J-P. Birabeau and J.M.A. Guérin, Patent N° 88 09820, Institut National De La Propriété Industrielle, 1993

[7] G. Orlandi et al., CERN-MT/93-13 (SM), paper presented at the 6th Workshop on RF Superconductivity, CEBAF, Newport News VA, USA, 1993

[8] R. Russo and S. Sgobba, “Influence of coating temperature on niobium films”, paper presented at the 8th Workshop on RF superconductivity, Abano Terme, Italy, 1997

[9] J.P. Turneaure et al., J. Supercond. 4 (1991) 341

[10] J. Halbritter, Z. Phys 266 (1974) 209

[11] C. Benvenuti et al., Physica B 197 (1994) 72

[12] C. Benvenuti et al., “Properties of copper cavities coated with different discharge gases”, paper presented at the 8th Workshop on RF superconductivity, Abano Terme, Italy, 1997